# Orthopositronium decay in gaseous, liquid, and solid helium[†]

J. B. Smith, Jr.,[†] J. D. McGervey, and A. J. Dahm

*Department of Physics, Case Western Reserve University, Cleveland, Ohio 44106*

Orthopositronium annihilation rates in liquid and solid helium up to 140 atm and in the liquid along the vapor-pressure curve up to the critical temperature have been measured and are analyzed in terms of the cavity model with a pressure-dependent radius. Two interdependent parameters of the model are the effective number of singlet annihilation electrons per helium atom $^1Z_{eff}$ for orthopositronium decay in helium gas and the orthopositronium–helium-atom scattering length $a_s$. Measurements of $o$-Ps in low-density helium gas at 77 K yielded $^1Z_{eff} = 0.116 \pm 0.004$ which is reasonably consistent with recently reported measurements at 300 K. With a low-density limit of $^1Z_{eff} = 0.125$, our pressure-dependent data are fit very well with an $a_s \simeq 1.15\ a_B$, while we do not obtain a good fit to the vapor-pressure measurements with the approximations used in the analysis. Sensitivity to the details of the model limits the accuracy of this result as a determination of $a_s$. We have also observed a nonlinearity in the $o$-Ps annihilation rate in He gas, and we have found $Z_{eff}$ for free-positron decay to be $3.86 \pm 0.04$ in the gas.

## I. INTRODUCTION

Early measurements of positronium annihilation in liquid helium revealed a long-lifetime component which could not be explained by a $2\gamma$ pick-off process for orthopositronium in a dense helium medium.[1,2] Ferrell[3] explained these results by proposing that a cavity, or bubble, formed around the Ps atom protecting it from the surrounding helium atoms. An excess electron in liquid,[4] solid,[5,6] or dense gaseous[7] helium forms a similar cavity, and this system has received extensive experimental and theoretical attention. A bubble is formed around a Ps atom because of the repulsive Pauli force between the electron of the Ps atom and the helium atomic core electrons; its size is determined by the balance between the external and surface tension pressure and the outward zero-point pressure of the Ps atom. The repulsive force excludes helium atoms from entering the bubble, and the annihilation rate is limited by the extent of the protrusion of the Ps wave function into the liquid.

Daniel and Stump[8] were the first to report a long $o$-Ps lifetime in dense helium gas, and Roellig and Kelly[9] made more extensive measurements which confirmed that Ps atoms form cavities in this medium as well. Further measurements of $o$-Ps decay in liquid helium at the vapor pressure were made by Liu and Roberts,[10] Manuzio,[11] Hautojärvi, Lopenen, and Rytsölä,[12] and by Roellig *et al.*[13] in rotating helium. The first quantitative measurement of a bubble parameter was made by Briscoe, Choi, and Stewart,[14] who determined the bubble radius from angular-correlation measurements on $p$-Ps in liquid helium. Triftshäuser *et al.*[15] extended this work to measure the pressure depen-

dence of the bubble radius in both liquid and solid helium and provided convincing evidence to support the bubble model. These latter data were analyzed by Hernandez and Choi,[16] who recalculated the radii by taking into account the finite potential well presented to the Ps atom by the liquid and examined the thermalization times for the ground state of the bubble to form.

We undertook this work to gain a better understanding of the overlap of the Ps wave function with the liquid, the pickoff rate in the liquid, and the bubble model as applied to positronium. In the analysis of our data we use three parameters: a pressure dependent surface tension, the effective number of electrons per helium atom for singlet annihilation in low-density helium-gas $^1Z_{eff}(0)$, and the low-energy positronium–helium-atom scattering length $a_s$. Since theoretical estimates of the pressure dependence of the surface tension and of the scattering length were in disagreement, and there was a large variance in the measured values of $^1Z_{eff}$ at the time this analysis was first undertaken, we measured the $o$-Ps pickoff rate as a function of density in helium gas at 77 K to reduce the number of uncertain parameters in our analysis. The free-positron decay rate in helium gas was also extracted from the data. A review of free-positron and $o$-Ps decay in gaseous and liquid helium has been given by Fraser.[17] Coleman *et al.*[18] have given a more recent summary of the gaseous data at 77 and 300 K, which does not include the results of Canter *et al.*[19]

Recent measurement of the pressure dependence of the $o$-Ps lifetime in liquid helium at 4.2 K was reported by Hautojärvi *et al.*[20] Our measurements are more extensive, and our analysis differs from theirs. We are also aware of unpublished mea-

surements of $o$-Ps lifetimes in liquid and solid helium under pressure.[21,22]

In Sec. II, we discuss our experimental apparatus and calibration, and our data are presented in Sec. III. The cavity model is presented and used to analyze the data in Sec. IV. The limitations of the cavity model and the variation of the measured scattering length with bubble parameters are discussed in Sec. V. Our conclusions are given in Sec. VI.

## II. EXPERIMENTAL APPARATUS AND CALIBRATION

The positron source was 2 $\mu$Ci of $^{22}$Na sealed between 3.8-$\mu$m mylar foils. Lifetimes were measured by a fast-slow coincidence system, using XP1021 photo multiplier tubes and 5.1-cm diameter Naton 136 scintillators, one of which was 7.6 cm long, and the other 3.8 cm long. The time spectrum was measured by an Ortec time-to-pulse-height converter (Model 437) whose output went to a 512 channel multichannel analyzer. The calibration, which was about 0.8 nsec per channel, was obtained by using pulses from a Hewlett Packard function generator (Model 3310A) and a 32-nsec delay box (EGG) whose uncertainty was 0.2 nsec. The calibration was checked by measuring the random coincidence rate per channel in the time spectrum and comparing it with the rate expected on the basis of the calibration and the single counting rates in each detector; the calibration was later rechecked by using an Ortec (Model 462) time calibrator.

Two experimental chambers of the following descriptions were used: a stainless steel sphere, 2.86-cm i.d. and 3.18-cm o.d., for measurements in condensed helium and in gaseous helium at densities above 100 amagats, and a cylindrical brass container, 10.2-cm i.d., 11.1-cm o.d., and 11.4 cm in length, for measurements in helium gas at lower densities. These chambers were sealed to the fill line with an indium "O" ring. The source was held at the center of the chambers with a BeCu wire. The 1-mm i.d. fill capillary was separated from the helium by a vacuum, and a heater wire was inserted into the entre length of the capillary. A copper plug was silver soldered into the bottom of the stainless steel chamber, and the chamber was coated with expandafoam. This design along with heating of the capillary insured that helium crystals grew from the bottom of the chamber as the temperature was lowered through the melting point at constant pressure, and that the crystals were completely grown before solid helium plugged the fill capillary. Measurements were made on crystals grown at constant density

by closing off the gas supply as a check on the solid helium density. The helium gas for the gas runs was purified by passing it through a zeolite filled stainless steel chamber submersed in liquid helium at 4.2 K. The scintillators were placed against the outside of the dewars, which were 4.8- and 14-cm o.d. respectively for the smaller and larger experimental chambers. Approximately $(2-3) \times 10^5$ counts were taken for each run. Additional details of the apparatus are given by Smith.[23]

## III. RESULTS

### A. Gaseous helium at 77 K

In analyzing our data, the measured background rate is first subtracted, and the annihilation rate versus time curves are then fit with two exponentials representing free positron and $o$-Ps annihilation rates. The free-positron annihilation decay rate was extracted from the data for atomic densities in the range $22 < n < 84$ amagats.[24,25] Our measured value for the free-positron decay rate is $\lambda_1 = (0.776 \pm 0.008)n$ $\mu$sec$^{-1}$ corresponding to a $Z_{eff}$ for free positrons of $3.86 \pm 0.04$. This value is reasonably consistent with the value of $Z_{eff} = 3.94 \pm 0.02$ from 300-K measurements reported by Coleman et al.[18]

Our measurements of the $o$-Ps annihilation rate are plotted as a function of atomic density in Fig. 1. The 77-K data of Roellig and Kelly[9] are shown for comparison. The solid line represents the results of Coleman et al. and corresponds to an effective number of electrons per helium atom for singlet annihilation of $^1Z_{eff} = 0.1252 \pm 0.0008$. The
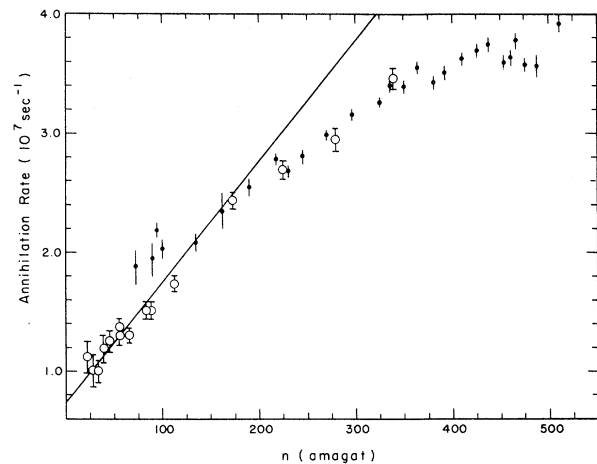


FIG. 1. Ortho-positronium annihilation rates versus density in helium gas at 77 K. The circles are data from the present work, and the solid points are taken from Roellig and Kelly.[9] The solid line represents the value $^1Z_{eff} = 0.125$ from Coleman et al.[18]

data show a definite nonlinearity for densities above 180 amagats, and the data at densities below this value are fitted with an annihilation rate[26] of $\lambda_2 = [7.24 + (0.093 \pm 0.003)n]$ $\mu\text{sec}^{-1}$ where the vacuum annihilation rate[27] of $\lambda_v = 7.24 \times 10^6$ $\text{sec}^{-1}$ is given infinite weight. The slope of $\lambda_2$ vs $n$ corresponds to $^1Z_{\text{eff}} = 0.116 \pm 0.004$.

### B. Liquid and solid helium

Measurements on $o$-Ps were taken as a function of pressure up to 140 atm at 1.4, 1.7, and 4.2 K, and along the coexistence curve up to 5.177 K. The annihilation rates under applied pressure are given in Table I. The melting pressures at 1.4, 1.7, and 4.2 K are respectively 25.74, 28.4, and 141 atm. Since the results at 1.4 and 1.7 K are nearly identical, we have plotted the annihilation rates only at 1.7 and 4.2 K as a function of pressure in Figs. 2 and 3 respectively. The vapor pressure measurements versus temperature are presented in Fig. 4, and the data of Hautojärvi, Lopenen, and Rytsölä[12] are included for comparison.

### IV. DATA ANALYSIS WITH THE CAVITY MODEL

We will assume that a spherical cavity of radius $R$ is formed about a Ps atom in condensed helium with a density profile given by

$$\rho = 0, \quad r < R \, ,$$
$$\rho = \rho_0, \quad r > R \, , \tag{1}$$

where $\rho_0$ is the equilibrium helium density at $r \gg R$. The Ps atom is treated as a hard sphere of radius equal to the scattering length $a_s$. The helium is then represented by a potential barrier given by

$$V = 0, \quad r < R - a_s \, ,$$
$$V = V_0, \quad r > R - a_s \, . \tag{2}$$

The probability $P_e$ that the center of mass of the Ps atom is external to the cavity, $r_{\text{c.m.}} > R$, is calculated, and the annihilation rate of $o$-Ps is written as

$$\lambda_2 = \lambda_v + P_e \lambda_e \, , \tag{3}$$

where $\lambda_e$ is the probability that pickoff occurs in a helium medium of density $\rho_0$. In writing Eq. (3) we have neglected the finite size of the Ps atom and have equated the coordinate of the positron with the center-of-mass coordinate of the Ps atom. It is implicitly assumed that the pickoff probability for $r_{\text{c.m.}} \lesssim R$, which we have neglected, is cancelled by an overestimate of the pickoff probability for $r_{\text{c.m.}} \gtrsim R$. All further discussion of the validity of our assumptions and of the parameters which we introduce into our model will be deferred until the next section.

The radius of the cavity is determined by minimizing the total energy which we write as

$$E = \hbar^2 k^2 / 2m + 4\pi R^2 \sigma + p(\tfrac{4}{3}\pi)R^3 \, . \tag{4}$$

Here $m$ is the mass of the Ps atom, $\sigma$ is the surface tension, $p$ is the externally applied pressure,

TABLE I. Annihilation rates of orthopositronium in condensed helium as a function of pressure.

| T = 1.4 K | | T = 1.7 K | | T = 4.2 K | |
|---|---|---|---|---|---|
| Pressure (atm) | Rate ($10^7$ sec$^{-1}$) | Pressure (atm) | Rate ($10^7$ sec$^{-1}$) | Pressure (atm) | Rate ($10^7$ sec$^{-1}$) |
| 4.50 | 1.33 ± 0.06 | 5.10 | 1.38 ± 0.07 | 1.0 | 1.05 ± 0.02 |
| 10.03 | 1.69 ± 0.07 | 10.03 | 1.45 ± 0.06 | 5.17 | 1.32 ± 0.05 |
| 14.80 | 1.56 ± 0.07 | 14.97 | 1.63 ± 0.06 | 9.86 | 1.50 ± 0.05 |
| 19.90 | 1.79 ± 0.06 | 20.07 | 1.68 ± 0.06 | 14.97 | 1.52 ± 0.05 |
| 23.47 | 1.88 ± 0.06 | 25.00 | 1.89 ± 0.06 | 20.14 | 1.72 ± 0.05 |
| 27.55 | 1.98 ± 0.06 | 31.97 | 2.14 ± 0.07 | 25.00 | 1.77 ± 0.05 |
| 41.33 | 2.27 ± 0.05 | 42.69 | 2.24 ± 0.07 | 29.76 | 1.88 ± 0.05 |
| 64.80 | 2.64 ± 0.05 | 49.80 | 2.36 ± 0.07 | 40.31 | 2.12 ± 0.05 |
| 78.74 | 2.84 ± 0.06 | 56.46 | 2.43 ± 0.06 | 55.10 | 2.24 ± 0.05 |
| 97.48 | 3.11 ± 0.06 | 64.46 | 2.55 ± 0.07 | 78.91 | 2.64 ± 0.05 |
| 119.39 | 3.36 ± 0.05 | 70.02 | 2.67 ± 0.07 | 99.49 | 2.81 ± 0.05 |
| 128.41 | 3.49 ± 0.07 | 78.74 | 2.80 ± 0.06 | 119.73 | 2.92 ± 0.05 |
| | | 97.82 | 2.94 ± 0.07 | 137.0 | 3.18 ± 0.07 |
| | | 118.88 | 3.33 ± 0.06 | | |
| | | 129.08 | 3.49 ± 0.07 | | |
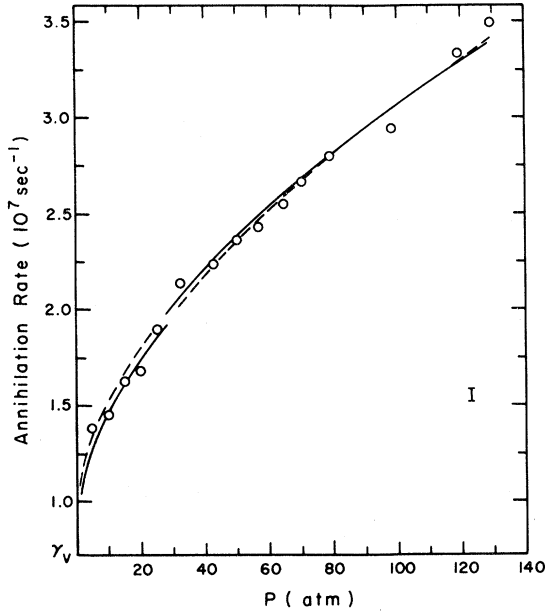
FIG. 2. Ortho-positronium annihilation rates versus pressure in condensed helium at 1.7 K. The solid and dashed lines are theoretical curves for $\sigma = \sigma(p)$ and $\sigma = \sigma_0$, respectively, with $^1Z_0 = 1.27$ and $a_s = 1.15\ a_B$. The breaks in the curves occur at the melting point where there is a surface tension and density discontinuity.
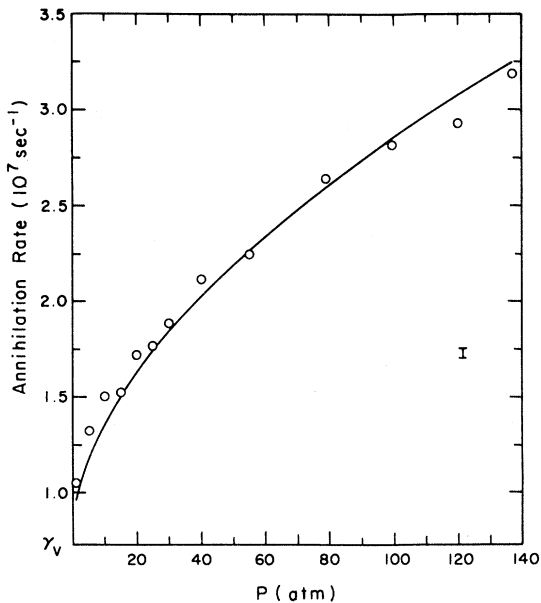


FIG. 3. Ortho-positronium annihilation rates versus pressure in liquid helium at 4.2 K. The solid line is the theoretical curve with $^1Z_0 = 1.26$ and $a_s = 1.15\ a_B$.
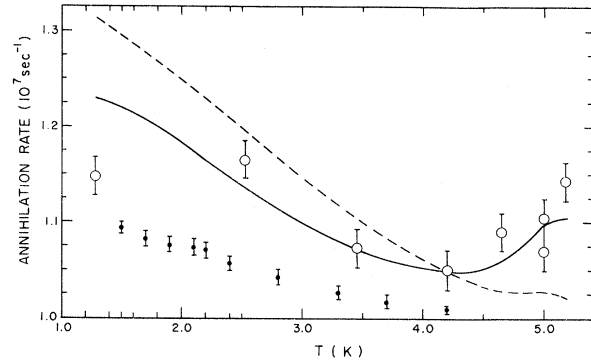


FIG. 4. Ortho-positronium annihilation rates versus temperature along the coexistence curve. The circles are data from the present work, and the solid points are taken from Hautojärvi et al.[12] The theoretical curves with $a_s = 1.15\ a_B$ are given by the solid line for $\sigma = \sigma_0$, $^1Z_0 = 0.188$, and by the dashed line for $\sigma = 1.7\ \sigma_0$, $^1Z_0 = 0.140$.

and $k$ is the Ps center-of-mass wave number. We may write $k$ as $k = x\pi/(R - a_s)$, where the value of $x$ is unity for an infinite potential $V_0$. We minimize $E$ with $x = 1$, find $R$, use the value of $R$ and the theoretical barrier height $V_0$ to determine a new value of $x$, and repeat the process to find a converging value of $x$. Given $x$ and $V_0$, $P_e$ is easily determined.[19]

The values of $\sigma$ and $V_0$ used in Eq. (4) are pressure dependent. We have used theory to scale $\sigma$ according to[28]

$$\sigma(p) = \sigma_0 n(p)s(p)/n_0 s_0 , \qquad (5)$$

where $n$ is the atomic density, $s$ is the velocity of sound, and the subscript $o$ refers to vapor pressure values. The measured equilibrium surface tension values were used along the vapor pressure curve.[29-31] For $V_0$ we use the Wigner-Seitz potential barrier calculated by Jortner et al.[32] They used the Wigner-Seitz method with an idealized pseudopotential given by

$$V = \infty, \quad r < a_s ,$$
$$V = 0, \quad r > a_s . \qquad (6)$$

to describe the Ps-He interaction.

The c.m. wave function is required to vanish at $r = a_s$ and to have a vanishing first derivative on the Wigner-Seitz sphere at radius $r_s = (3/4\pi n)^{1/3}$. This leads to

$$\psi = N[\sin k_0(r - a_s)]/k_0 r , \qquad (7)$$

where $N$ is a normalization constant, and an equa-

tion for the wave number $k_0$ of the lowest state of a free Ps atom in condensed helium which is

$$\tan k_0(r_s - a_s) = k_0 r_s . \tag{8}$$

The Wigner-Seitz potential barrier is

$$V_{WS} = \hbar^2 k_0^2 / 2m . \tag{9}$$

We write the pickoff rate in the condensed medium in terms of $^1Z_{eff}$ as

$$\lambda_e = 4\pi r_0^2 cn \, {}^1Z_{eff}(n) , \tag{10}$$

where $r_0$ is the classical electron radius, and $c$ is the velocity of light.[17] Since the $o$-Ps helium inter-action is repulsive, $o$-Ps atoms will avoid the volume occupied by helium atoms. An increase in density, or equivalently in the excluded volume, will cause an increase in the amplitude of the $o$-Ps wave function and an enhancement in the value $^1Z_{eff}$. Ferrell obtained an expression for this enhancement in an unpublished calculation.[33] He normalized the Ps wave function within a Wigner-Seitz sphere and used the model pseudopotential subsequently used by Jortner *et al.* to determine the potential barrier. The normalization procedure

$$1 = \int_{a_s}^{r_s} \psi^*(r)\psi(r)4\pi r^2 \, dr , \tag{11}$$

with $\psi(r)$ given by Eq. (7), leads to

$$N^2 = (3/4\pi r_s^3)\left( \frac{\frac{2}{3}k_0^2 r_s^3}{(r_s - a_s) - (2k_0)^{-1}\sin 2k_0(r_s - a_s)} \right)$$

$$= nF(n). \tag{12}$$

For $r_s \gg a_s$, Eq. (8) shows that $k_0 r_s \ll 1$; therefore, in this case, $\sin 2k_0(r_s - a_s) \simeq 2k_0 r_s - 8k_0^3 r_s^3/6$, and $F(n) \to 1$.

The pickoff rate varies as $|\psi|^2$ so that we may write

$$^1Z_{eff}(n) = {}^1Z_0 F(n) . \tag{13}$$

where $^1Z_0$ is the low-density limit of $^1Z_{eff}$ measured in helium gas. For calculational convenience we rewrite $F(n)$ with the use of Eq. (8) and trigonometric identities as

$$F(n) = \frac{2}{3} \frac{1 + k_0^2 r_s^2}{1 - (a_s/r_s)[1 + (k_0^2 r_s^2)^{-1}]} . \tag{14}$$

The value of $k_0 r_s$ varies from 1.22 to 1.39 in the pressure range 0–130 atm at 1.7 K. The variation of $^1Z_{eff}$ with density as $(1 - a_s/r_s)^{-3}$ suggested by Ferrell[3] was the low-density limit $a_s/r_s \ll 1$ of Eq. (12).

We used a series of scattering lengths in the square-well model and determined a value of $^1Z_0$ for a best fit to the pressure dependent data in each case. Nearly identical curves were generated by different sets of $^1Z_0$ and $a_s$, and the values of

$^1Z_0$ for the two sets of data at 1.7 and 4.2 K agree. A plot of $^1Z_0$ vs $a_s$ has only a slight negative curvature and in the range $0.95 \, a_B \lesssim a_s \lesssim 1.39 \, a_B$ (Bohr radii) is fit well with the empirical relation $^1Z_0 = 1.09 \, a_s/a_B$. The value of $a_s$ corresponding to $^1Z_0 = 0.125$ is $a_s = 1.15 \, a_B = 0.61$ Å. The solid curves in Figs. 2 and 3 are theoretical curves for $^1Z_0 = 0.127$ and 0.126 respectively and with $a_s = 1.15 \, a_B$. The best fit to the vapor pressure data with $a_s = 1.15 \, a_B$ is given with $^1Z_0 = 0.188$, and the solid curve in Fig. 4 is the theoretical curve for these values.

## V. DISCUSSION

### A. Helium gas

Our low-density measurements of the $o$-Ps annihilation rate in helium gas at 77 K, shown in Fig. 1, yield a value of $^1Z_{eff} = 0.116 \pm 0.004$, slightly lower than the recent values of $0.1252 \pm 0.0008$ and $0.129 \pm 0.006$ given respectively by Coleman *et al.*[18] and Canter *et al.*[19] Prior measurements are discussed by Fraser[17] and by Coleman *et al.* We use the most precise value of Coleman *et al.* in analyzing the data in condensed helium.

At high densities our measurements are in agreement with the 77 K data of Roellig and Kelly[9] although their low-density results appear to be in error. A definite nonlinearity sets in at about 180 amagats. Fraser[17] suggested, *ad hoc*, such a nonlinearity to explain the results of Roellig and Kelly. Leung and Paul[34] found a non-linearity at lower densities, but their data fall distinctly below the results of other workers. This is perhaps a consequence of difficulties they encountered in sealing their experimental cell at 77 K. The nonlinearity probably results from multiple scattering effects and may be a precursor to bubble formation as-suggested by Fraser. Roellig and Kelly attribute the deviation from a smooth curve at about 375 amagats to bubble formation.

### B. Liquid and solid helium

Our measured annihilation rates at 4.2 K are in excellent agreement with the unpublished results of Kelly[21] and are about 3% larger than the data of Hautojärvi *et al.*[20] Kelly's measurements at 1.4 K show a much weaker pressure dependence and are in serious disagreement with our results. The more precise annihilation rates of Hautojärvi, Lopenen, and Rytsölä[12] along the vapor pressure curve are smaller than our results by about 5%, and the less precise annihilation rates of Manuzio are larger by 20%. A 5% difference in the total annihilation rate at $\lambda = 1.1 \times 10^7$ sec$^{-1}$ is equivalent

to a 13% difference in the $2\gamma$ pickoff rate. The vapor pressure data of Hautojärvi *et al.* are best fit with our model with $a_s = 1.15\,a_B$ and $^1Z_0 = 0.150$. The bubble radius increases with $T$ as the surface tension decreases and reaches a calculated maximum of 18.7 Å at $T = 4.4$ K leading to a minimum in the annihilation rate.

The single square-well model with the parameters used obviously fails to fit all of the data. It gives a good fit to the pressure dependent data, but a much poorer fit to the vapor pressure measurements, and the value of $^1Z_0$ required to fit the latter is 50% larger. For a given value of $^1Z_0$ and $a_s$ the calculated pickoff rate depends critically on the functional dependence of $\sigma$, $V_0$, and $F(n)$ on the density. Whereas most of the measurements on electron bubbles in liquid and solid helium depend in first order on the radius and to second order on the potential barrier, the pickoff rate of $o$-Ps depends critically on the amplitude of c.m. wave function at the surface and therefore on the value of $V_0$. The $o$-Ps pickoff rates are also much more sensitive to the surface profile than are experiments on electron bubbles.

We will examine the variation of the pickoff rate with the parameters introduced into the model. Then we will discuss a more realistic surface profile and the accuracy of the parameters introduced into the model. We will comment on the limitations of the bubble model in calculating $o$-Ps pickoff rates and finally compare our value of the scattering length with other values deduced from pickoff rates in gaseous and liquid helium.

### C. Variation of the pickoff rates with model parameters

The dependence of the pickoff rate on the model parameters can be observed by writing the pickoff rate as

$$\lambda_2 - \lambda_v = 4\pi r_0^2 c n\,{}^1Z_0 P_e F(n) \ . \tag{15}$$

A smaller value of $V_0$ or larger value of $\sigma(p)$, which constricts the bubble, both increase $P_e$. The effect of increasing the scattering length is to increase $F(n)$ and to decrease $P_e$ as a result of an enhanced $V_0$ and the fact that the potential barrier at $R - a_s$ is moved further from the surface. While these effects partially cancel, the net effect of increasing $a_s$ is to decrease the pickoff rate, thus requiring a larger value of $^1Z_0$ to fit the data.

### D. Surface profile

The surface profile, which we have approximated by a step function, has been calculated by a number of workers for the free surface of liquid

helium at $T = 0$. The surface tension is minimized with an assumed density profile. Most authors[28,35-40] use a symmetric profile and obtain values of the surface width ranging from 0.7 to 3.0 Å. Chang and Cohen[41] obtained a lower surface tension by relaxing the symmetry condition and found healing lengths of 0.7 Å on the outside of the surface and 2.0 Å on the interior compared to a total width of 2 Å for their symmetric profile. Padmore and Cole[42] have also used an asymmetric profile and quote a free surface thickness (10%–90% density) of 5.9 Å. These workers specifically examine the surface of the electron bubble and find that the effect of the surface curvature is negligible. They also find only a 10% tightening of the surface from the zero-point pressure of the electron, $p_{zp} \simeq 5$ atm. Some additional tightening will occur at higher pressures, but the ratio of the surface thickness to the bubble radius will probably not change much. Regge[39] found a damped oscillatory density profile at the surface with a period approximately equal to an atomic spacing. Surface calculations by a number of authors are assessed by Liu, Kalos, and Chester.[43] These authors show that the surface density oscillations are weak and therefore will not appreciably affect the pickoff rates.

### E. Validity of bubble parameters

One might hope to be able to determine the correct values and pressure dependence of the parameters $\sigma$ and $V_0$ by comparing theoretical and experimental quantities associated with electron bubbles in liquid helium. However, the bubble radius, which is the parameter most often deduced from experiment, depends only weakly on $V_0$ and $\sigma$; $[R \simeq (\sigma + \frac{1}{2}pR)^{-1/4}]$. Padmore and Cole discuss the electron bubble in some detail and point out that the substantial surface thickness and the application of classical hydrodynamics on the scale of Angstroms in deducing bubble radii from experimental results will lead to errors of 1–2 Å. Further, with a diffuse surface different experiments will measure different radii. Nevertheless, we might expect the qualitative variation of the bubble radius with pressure to be accurately calculable.

A simple optical model applicable to very low atomic densities yields a barrier[44]

$$V_0 = 2\pi\hbar^2 n a_s/m \ . \tag{16}$$

Tankersley[45] performed a multiple scattering calculation and obtained corrections to Eq. (16) in terms of the fluid structure factor. His high density approximation is given by

$$V_{\mathrm{ms}} = (2\pi\hbar^2 n a_s/m)[1 + (4.5\pi n)^{1/3}a_s] \ . \tag{17}$$

Burdick[46] used a lattice model to calculate the barrier, and his results, not given in closed form, are slightly less than $V_{WS}$. The four potentials are shown as a function of pressure at 4.2 K for $a_s = 1.17\ a_B$ in Fig. 5.

Measurements of the electron barrier in liquid helium span the range[47] 0.82–1.3 eV compared to the theoretical values of 0.94–1.3 eV. Broomall and Onn[48] have measured the pressure dependence of $V_0$ for electrons in helium by a rather indirect method in which the barrier is extracted from a prefactor of an exponential plot. The magnitude of their measurements are in agreement with the Wigner-Seitz model, although their pressure dependence is weaker than the predictions of this model.

Most analyses of the electron bubble were given prior to the publication of Tankersley's work and use the Wigner-Seitz potential barrier. Miyakawa and Dexter[49] analyzed the electronic energy levels in the bubble from the data of Northby-Zipfel-Sanders[50] with a square-well model. They scaled the surface tension as $ns$ and found $V_0 = 0.95$ eV at zero pressure, in agreement with $V_{ms}$, but could obtain the pressure dependence by scaling $v_0$ with either the optical potential, Eq. (16), or the Wigner-Seitz model. Schwarz[51] uses a simple square-well model and obtains good agreement between the calculated pressure dependent radius and the radii as measured by vortex trapping experiments when scaling the surface tension as $ns$, but obtains better agreement with the radii deduced from mobility experiments when taking $\sigma$ to be a constant equal to the value at the vapor pressure $\sigma_0$. Springett, Cohen, and Jortner[52] and Shih and Woo[53] have both computed the bubble radius as a function of pressure using $V_{WS}$ and variational methods as opposed

to a simple square-well model. Both papers use an assumed exponential form for the electronic wave function and use sharp surface profiles. Springett et al. neglect the long-range electron-helium polarization, but use a large surface tension at the vapor pressure which constricts the bubble and makes it less compressible. Springett et al. scale $\sigma$ as $ns$ while Shih and Woo calculate the surface tension and find it to be nearly pressure independent. Both sets of authors obtain nearly the same pressure dependence of the bubble radius. The value of $\sigma(p)$, Eq. (5), increases by a factor of 4.5 from 0 to 100 atm. We conclude that on the basis of the present experimental and theoretical work on electron bubbles in helium it is not possible to distinguish the correct form of $V_0$ or $\sigma(p)$.

We have analyzed our data with a pressure independent surface tension, $\sigma = \sigma_0$, and $a_s = 1.15\ a_B$, and the "best-fit" values of $^1Z_0$, given in Table II, are increased by 16% and 6% respectively at 1.7 and 4.2 K. Equivalently, for a given $^1Z_0$, the best fit values of $a_s$ would be less by these percentages. The theoretical curve for $\sigma = \sigma_0$ at 1.7 K is given as a dashed line in Fig. 2, while there is little effect on the annihilation rates at 4.2 K because of the small value of $\sigma_0$. It may be observed from the discontinuity in the dashed curve at the melting point that a change in density at constant pressure and surface tension (nearly constant $R$), leads to a decrease in the annihilation data. In Fig. 6 we plot the square well radius $R - a_s$ vs pressure for $\sigma = \sigma(p)$ and $\sigma = \sigma_0$ for comparison with the angular correlation experiments as analyzed by Hernandez and Choi.[16] Their experimental values would be somewhat reduced if the data were analyzed with a smaller potential consistent with a smaller scattering length, and it is unclear which set of curves would give a better fit to the bubble radii. The use
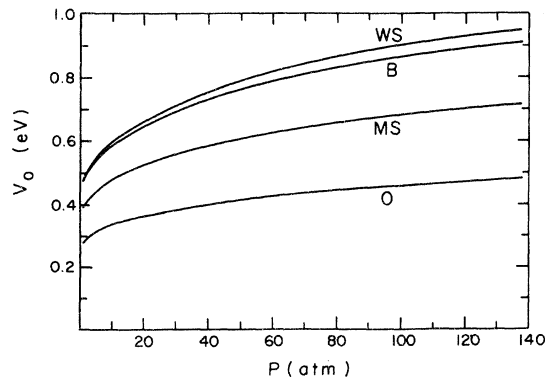


FIG. 5. Potential barriers for various approximations versus pressure at 4.2 K for $a_s = 1.17\ a_B$. The notation is: O, optical potential Eq. (16); MS, multiple scattering potential, Eq. (17); B, Burdick's potential; and WS, Wigner-Seitz potential.

TABLE II. The quantity $^1Z_0$ given by the best fit to the pressure dependent annihilation rates for various scattering lengths and bubble parameters which are A: $V_0 = V_{WS}$, $\sigma = \sigma(p)$, Eq. (5); B: $V_0 = V_{WS}$, $\sigma = \sigma_0$; C: $V_0 = V_{WS}$, $\sigma = 1.7\sigma_0$; D: $V_0 = V_{ms}$, $\sigma = \sigma(p)$, Eq. (5).

| Bubble parameters | $a_s/a_B$ | 1.7 K | 4.2 K |
|---|---|---|---|
| A | 0.95 | 0.104 | 0.103 |
|   | 1.15 | 0.127 | 0.126 |
|   | 1.25 | 0.137 |  |
|   | 1.39 | 0.152 | 0.151 |
|   | 1.61 | 0.173 | 0.172 |
| B | 1.15 | 0.147 | 0.133 |
| C | 1.15 | 0.140 | 0.132 |
| D | 1.17 |  | 0.083 |
|   | 1.39 |  | 0.085 |
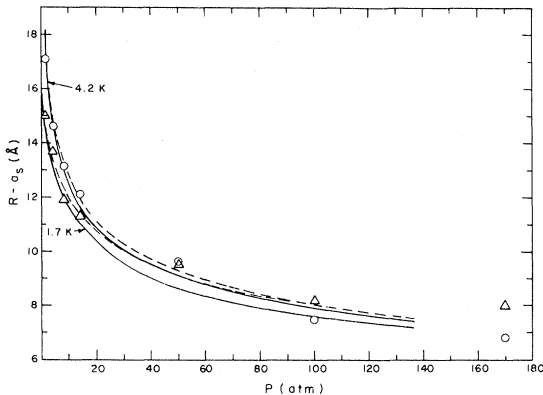
FIG. 6. Square-well radius vs pressure. The symbols are experimental data as analyzed by Hernandez and Choi[16]: $0$—4.2 K, $\triangle$—1.7 K. The solid and dashed lines are square well radii with $\sigma = \sigma(p)$ and $\sigma = \sigma_0$, respectively, and $a_s = 1.17 \, a_B$.

of a constant surface tension leads to a poorer agreement between the values of $^1Z_0$ obtained from the 1.7 and 4.2 K data, and a compromise value of $^1Z_0 = 0.140$ gives only a moderate fit to the data.

We have also used a fudge factor and set $\sigma = 1.7 \, \sigma_0$,[54] and the corresponding values of $^1Z_0$ are given in Table II. This factor increases the annihilation rates at low pressures and has little effect at high pressures. The vapor pressure data could not be fit with this parameter as can be observed from Fig. 4, and the fit to the pressure dependent data at 1.7 K was considerably worse.

Finally, Ferrell's calculation of the density dependence of the pickoff rate is based on the Wigner-Seitz model. If $V_{WS}$ is too large, then $F(n)$ given by Eq. (12) is overestimated and $P_e$ is underestimated. These errors partially cancel in calculating the pickoff rate. We analyzed the 4.2 K data with the multiple scattering potential for $a_s = 1.17$ and $1.39 \, a_B$. The resultant values of $^1Z_0$, given in Table II, are very small and insensitive to changes in $a_s$. This is probably a result of either too small a value of $V_0$ and/or too large a value of $F(n)$ with an addition rather than a cancellation of errors. We believe that the large value of $^1Z_0$ and the poor fit to the data at the vapor pressure result in part from the application of the Wigner-Seitz model in calculating $V_0$ and $F(n)$ at low densities.

### F. Limitations of the model

Aside from uncertainties in the model parameters, there are inherent limitations associated with the simple model employed here. The c.m. wave function of the positronium decays as $e^{-r/l}$

into the liquid, where $l \simeq 3$ Å is less than the interatomic separation. While such a simple form of the wave function may be adequate to calculate the radius of the bubble, it is too coarse for an exact determination of the pickoff rate. We have treated the Ps atom as a point particle, assuming that the neglect of pickoff for $r = R - \delta$ will be cancelled by an overestimate of pickoff at $r = R + \delta$, where $r$ is the c.m. coordinate. This cancellation for a square well is incomplete since $|\psi(R - \delta)|^2 > |\psi(R + \delta)|^2$. The situation is much worse for an asymmetric surface profile with a width which is on the order of one-third of the bubble radius. Another effect which is neglected is the polarization of the Ps atom at the surface. Some polarization is expected since the electron He interaction is repulsive at short range while the positron-He interaction is attractive.

### G. Comparison of scattering lengths

Our value of the scattering length deduced from the pressure dependent data, $1.00 \, a_B \leq a_s \leq 1.15 \, a_B$ may be compared with the value $0.95 \, a_B \leq a_s \leq 1.5 \, a_B$ obtained by the Helsinki group[12,20] who measured $o$-$Ps$ annihilation rates along the vapor pressure curve from 1.3 to 4.2 K and from 1–60 atm at 4.2 K. While there is some disagreement in the measured annihilation rates, the principal difference between their work and ours is the method of analysis. The Helsinski group uses the square-well model with the following differences: the potential barrier is located at $R$ as opposed to $R - a_s$, and the form $^1Z_{eff} = ^1Z_0 \, (1 - a_s/r_s)^{-3}$ is used with $a_s = 1.872 \, a_B$ and $^1Z_0 < 0.02$. They then determine $P_e$ from the data and use an expression which relates $P_e$ to $V_0$ and $R$ along with an analysis of the angular correlation data of Triftshäuser et al.[15] to determine $R$ and $V_0$. The scattering length is related to $V_0$ by the optical approximation. Their smaller values of $^1Z_{eff}$ yield small potential barriers and partially cancel the error introduced in using the optical approximation to obtain the scattering length. The use of the two complementary sets of data, angular correlation and lifetime measurements, should give an accurate value of the scattering length in a more exact model.

Orthopositronium scattering lengths have also been extracted from lifetime measurements in dense helium gas. These values are quoted as $a_s = 1.45 \, a_B$ for $^4$He,[19] and $a_s = 1.34 \, a_B$ for $^3$He.[55] The cavities in the vapor have an even more diffuse surface than in the liquid and energetic helium atoms may penetrate the cavities so that their analysis suffers from some of the same difficulties as ours. In addition, cavities in the vapor are expected to have a distribution of shapes and sizes[56]

and the ground state will not be the only occupied state.[57] Hernandez[57] has estimated the scattering length as approximately 1.5 $a_B$ by examining both the o-Ps annihilation rates and the density and pressure dependence of cavity formation in $^4$He gas.

Our experimental value is less than the most recent theoretical value[58] of 1.39 $a_B$, which represents an upper limit for the model used in the calculation.

## VI. CONCLUSIONS

The simple square cavity model with Wigner-Seitz calculations for $V_0$ and $^1Z_{eff}(n)$ is inadequate to analyze the data throughout the density range investigated. The sensitivity of the pickoff rate to the potential barrier and surface profile requires a more exact model for analysis along with a theory for $^1Z_{eff}$ which takes into account the correlations of atoms in the liquid as opposed to a lattice calculation. In the high-density region where the Wigner-Seitz model is a better approximation, the analysis used here fits the experimental data with $a_s = 1.15$ $a_B$ and $\sigma$ scaled as $ns$. The data require a smaller scattering length if $\sigma$ has a weaker density dependence. The value of $a_s \simeq 1.15$ $a_B$ is quoted with very limited precision, but the data suggest that the scattering length is less than the lowest theoretical value or values obtained from experiments in helium gas.

## ACKNOWLEDGMENTS

*Work supported in part by the NSF and the U. S. Atomic Energy Commission.

†Present address: Case Western Reserve University, Medical School, Cleveland, Ohio 44106.

[1] D. A. L. Paul and R. L. Graham, Phys. Rev. 106, 16 (1957).

[2] J. Wackerle and R. Stump, Phys. Rev. 106, 18 (1957).

[3] R. A. Ferrell, Phys. Rev. 108, 167 (1957).

[4] Two excellent reviews of ions in liquid helium are (a) K. W. Schwarz in Advances in Chemistry and Physics, edited by I. Prigogine and S. A. Rice (Wiley, New York, 1975), Vol. XXXIII, p. 1; and (b) A. Fetter, in The Physics of Liquid and Solid Helium, edited by K. H. Benneman and J. B. Ketterson (Wiley, New York, 1975). (c) See also B. E. Springett, Morrel H. Cohen, and Joshua Jortner, Phys. Rev. 159, 183 (1967).

[5] M. H. Cohen and J. Jortner, Phys. Rev. 180, 238 (1969).

[6] G. A. Sai-Halasz and A. J. Dahm, Phys. Rev. Lett. 28, 1244 (1972).

[7] J. Levine and T. M. Sanders, Jr., Phys. Rev. 154, 138 (1967).

[8] T. B. Daniel and R. Stump, Phys. Rev. 115, 1599 (1959).

[9] L. O. Roellig and T. M. Kelly, Phys. Rev. Lett. 18, 387 (1967).

[10] D. C. Liu and W. K. Roberts, Phys. Rev. 130, 2322 (1963).

[11] G. E. Manuzio, Nuovo Cimento 42, 342 (1966).

[12] P. Hautojärvi, M. T. Lopenen, and K. Rytsölä, J. Phys. B 9, 411 (1976).

[13] L. O. Roellig, T. Kelly, H. H. Madden, and J. McNutt, Proceedings of the Ninth International Conference on Low Temperature Physics, edited by J. G. Daunt, D. O. Edwards, F. J. Milford, and M. Yaqub (Plenum, New York, 1965), Vol. I, p. 195.

[14] C. V. Briscoe, S.-I. Choi, and A. T. Stewart, Phys. Rev. Lett. 20, 493 (1968).

[15] W. Triftshaüser, J. Legg, A. T. Stewart, and C. V. Briscoe, Proceedings of the Eleventh International Conference on Low Temperature Physics, edited by

J. F. Allen, D. M. Finlayson, and D. M. McCall (Univ. of St. Andrews Press, St. Andrews, Scotland, 1969), Vol. I, p. 304.

[16] J. P. Hernandez and S.-I. Choi, Phys. Rev. 188, 340 (1969).

[17] P. A. Fraser, in Advances in Atomic and Molecular Physics, edited by D. R. Bates and Immanuel Estermann (Academic, New York, 1968), Vol. 4, p. 63.

[18] P. G. Coleman, T. C. Griffith, G. R. Heyland, and T. L. Killeen, J. Phys. B 8, 1734 (1975).

[19] K. F. Canter, J. D. McNutt, and L. O. Roellig, Phys. Rev. A 12, 375 (1975).

[20] P. Hautojärvi, K. Rytsölä, P. Tuvinen, and P. Jauho, Phys. Lett. A 57, 175 (1976).

[21] T. M. Kelly, Ph.D. thesis (Wayne State University, 1966) (unpublished).

[22] K. F. Canter, J. D. McNutt, and L. O. Roellig (private communication).

[23] J. B. Smith, Ph.D. thesis (Case Western Reserve University, 1973) (unpublished).

[24] The atomic densities were obtained from the equation of state given by R. D. McCarty and R. B. Stewart, Progress in International Research in Thermodynamics and Transport Properties (Academic, New York, 1962).

[25] The amagat is defined as the STP density, $2.687 \times 10^{19}$ atoms/cm$^3$.

[26] A smaller value determined by attempting to fit all of the data to a linear curve was reported by J. B. Smith, J. D. McGervey, and A. J. Dahm, Proceedings of the Fourth International Conference on Positron Annihilation, Helsingør, Denmark (unpublished).

[27] M. A. Stroscio and J. M. Holt, Phys. Rev. A 10, 749 (1974).

[28] D. Amit and E. P. Gross, Phys. Rev. 145, 130 (1966). These authors have calculated the surface tension at $T = 0$, $p = 0$, to be equal to 0.7 $\hbar ns$.

[29] Surface tension values below 2 K were taken from K. R. Atkins and Y. Narahara, Phys. Rev. 138, A437 (1965), and above 2 K from J. F. Allen and A. D. Misener,

Proc. Camb. Philos. Soc. 34, 299 (1958). A linear extrapolation of the data of Allen and Misener to zero at the critical temperature was used for $T > 4.4$ K.

[30]Density values for the solid were taken from D. O. Edwards and R. C. Pandorf, Phys. Rev. 140, A816 (1965) and for the liquid under pressure from W. H. Keesom, *Helium* (Elsevier, New York, 1942), p. 240. At the vapor pressure density values for $T \leq 4.4$ K were taken from E. C. Kerr and R. D. Taylor, Ann. Phys. (N.Y.) 26, 292 (1964), and for $T > 4.4$ K from R. Berman and C. F. Mate, Philos. Mag. 3, 461 (1958).

[31]Values of the velocity of sound in the solid were taken from J. H. Vignos and H. A. Fairbank, Phys. Rev. 147, 185 (1966), and for the liquid from K. R. Atkins and R. A. Stasior, Can. J. Phys. 31, 1156 (1953).

[32]J. Jortner, N. R. Kestner, S. A. Rice, and M. H. Cohen, J. Chem. Phys. 43, 2614 (1965).

[33]This derivation was communicated to us by R. A. Ferrell.

[34]C. Y. Leung and D. A. L. Paul, J. Phys. B 2, 1278 (1969).

[35]R. Brout and M. Nauenberg, Phys. Rev. 112, 145 (1968).

[36]K. Hiroike, N. R. Kestner, S. A. Rice, and J. Jortner, J. Chem. Phys. 43, 2625 (1965).

[37]D. Pitts, Physica (Utr.) 42, 205 (1969). This author obtains an anomalously large value of $\simeq 12$ Å.

[38]R. M. Bowley, J. Phys. C 3, 2012 (1970).

[39]T. Regge, J. Low Temp. Phys. 9, 123 (1972).

[40]Y. M. Shih and C. W. Woo, Phys. Rev. Lett. 30, 478 (1973).

[41]C. C. Chang and M. Cohen, Phys. Rev. A 8, 1930 (1973).

[42]T. Padmore and M. W. Cole, Phys. Rev. A 9, 802 (1974).

[43]K. S. Liu, M. H. Kalov, and G. V. Chester, Phys. Rev.

B 12, 1715 (1975).

[44]W. Lenz, Z. Phys. 56, 778 (1929); J. Levine and T. M. Sanders, Jr., Phys. Rev. 154, 138 (1967). This potential follows from a special case of a more general scattering theory by L. L. Foldy, *ibid.* 67, 107 (1945).

[45]L. L. Tankersley, J. Low Temp. Phys. 11, 451 (1973).

[46]B. Burdick, Phys. Rev. 14, 11 (1965).

[47]For a summary of the experimental and theoretical values of the electron barrier in helium, see W. Schoepe and G. W. Rayfield, Phys. Rev. A 7, 2111 (1973).

[48]J. R. Broomall and D. G. Onn, *Proceedings of the Fourteenth International Conference on Low Temperature Physics*, edited by M. Krusius and M. Vuorio (North-Holland, Amsterdam, 1975), Vol. I, p. 439.

[49]T. Miyakawa and D. L. Dexter, Phys. Rev. A 1, 513 (1970).

[50]J. A. Northby and T. M. Sanders, Jr., Phys. Rev. Lett. 18, 1184 (1967); C. Zipfel and T. M. Sanders, Jr., in Ref. 15, Vol. I, p. 296.

[51]K. W. Schwarz, Ref. 4a.

[52]B. E. Springett, M. H. Cohen, and J. Jortner, Ref. 4c.

[53]Y. M. Shih and C. W. Woo, Phys. Rev. A 8, 1437 (1973).

[54]Some authors have used this fudge factor to fit experimental data on the electron bubble. See, for example, R. M. Ostermeier and K. W. Schwarz, Phys. Rev. A 5, 2510 (1972).

[55]K. F. Canter (private communication). This value is less than the value reported by M. Fishbein and K. F. Canter, Phys. Lett. A 55, 398 (1976) and results from the analysis of additional data.

[56]T. P. Eggarter, Phys. Rev. A 5, 2496 (1972).

[57]J. P. Hernandez (unpublished).

[58]R. J. Drachman and S. K. Houston, J. Phys. B 3, 1657 (1970).